Journal of Colloid and Interface Science 438 (2015) 39–46

Contents lists available at ScienceDirect

Journal of Colloid and Interface Science

www.elsevier.com/locate/jcis

Interaction of cyclic and linear Labaditin peptides with anionic and zwitterionic micelles

S.C. Barbosa [a], E.M. Cilli [b], L.G. Dias [a], C.A. Fuzo [a], L. Degrève [a], R.G. Stabeli [c], R. Itri [d], P. Ciancaglini [a,*]

[a] Departamento de Química, FFCLRP-USP, 14040-901 Ribeirão Preto, SP, Brazil
[b] Departamento de Bioquímica e Biotecnologia, IQ-UNESP-Univ. Estadual Paulista, Araraquara, SP, Brazil
[c] Centro de Estudos de Biomoléculas Aplicadas a Medicina (CEBio), Núcleo de Saúde (NUSAU), Universidade Federal de Rondônia (UNIR), Fundação Oswaldo Cruz – Fundação Oswaldo Cruz – Rondônia (FIOCRUZ), 76812-245 Porto Velho, RO, Brazil
[d] Departamento de Física Aplicada, Instituto de Física, IF-USP, São Paulo, SP, Brazil

ARTICLE INFO

Article history:
Received 5 July 2014
Accepted 17 September 2014
Available online 2 October 2014

Keywords:
Labaditin
Cyclic peptide
Circular dichroism
Fluorescence
Molecular dynamic

ABSTRACT

Conformational changes of the cyclic (Lo) peptide Labaditin (VWTVWGTIAG) and its linear analogue (L_1) promoted by presence of anionic sodium dodecyl sulfate (SDS) and zwitterionic L-α-Lysophosphatidylcholine (LPC) micelles were investigated. Results from λ_{max} blue-shift of tryptophan fluorescence emission combined with Stern–Volmer constants values and molecular dynamics (MD) simulations indicated that L_1 interacts with SDS micelles to a higher extent than does Lo. Further, the MD simulation demonstrated that both Lo and L_1 interact similarly with LPC micelles, being preferentially located at the micelle/water interface. The peptide–micelle interaction elicits conformational changes in the peptides. Lo undergoes limited modifications and presents unordered structure in both LPC and SDS micelles. On the other hand, L_1 displays a random-coil structure in aqueous medium, pH 7.0, and it acquires a β-structure upon interaction with SDS and LPC, albeit with structural differences in each medium.

1. Introduction

It is well established that cyclic peptides (CPs), which are more resistant to proteolytic degradation than their linear isomers [1–4], form internal hydrogen bonds that facilitate their membrane insertion [4,5]. In addition, the more restricted conformational flexibility of CPs leads to an enhancement of their affinity and specificity to receptors [2,4–7].

CPs belonging to the *Caryophyllaceae* group consist of 7–10 aminoacids with a high proportion of hydrophobic residues [8–12] being recently named as Orbitide [13]. Biobollein (9 residues) and Labaditin (10 residues), isolated from *Jatropha Multifida*, were the first CPs of this group of peptides described in the literature [8,14,15]. One recent review about *Jatropha species* presented 19 cyclic peptides isolated from this family [16]. In particular, it has been shown that Labaditin (VWTVWGTIAG), a highly hydrophobic CP from a popular plant known as Jarak gurita (Indonesia) and also Mana (Philippines) [15], has antibacterial and acetylcholinesterase activities [14]. Moreover, Labaditin inhibits the classical pathway of human complement activation *in vitro* [14,16]. It binds to aggregated and antigen-bound IgG, mostly blocking the antibody Clq acceptor site, which is restricted to IgG subclass IgGl [15,17].

Although the biological activity of CPs is well reported, the mechanism of action of such peptides on the molecular level is poorly comprehended. In this context, it is of importance to explore the role of hydrophobic and polar environment to the peptide affinity by mimicking the biological membrane. The hydrophobic medium certainly plays an important role in peptide partitioning [18–20], since many hydrophobic amino acid residues, especially aromatic ones, are favorably distributed in the aqueous/lipid membrane interface [21,22]. This might explain structural changes imparted by bioactive molecules in contact with the membrane as well as their regulation mechanisms [23].

In this work, we investigate the behavior of the cyclic peptide Labaditin (Lo) in comparison with its linear analog (L_1) when in contact with micelles as model membranes. Lysophosphatylcholine (LPC) and sodium dodecyl sulfate (SDS) micelles were chosen because LPC is structurally similar to PC-based lipids commonly found in mammalian cells [24], whereas the presence of negative net charge in SDS micelles may help us to understand how the surface charge in the bacterial membrane influences the peptide binding. Fluorescence spectroscopy and circular dichroism (CD) techniques were employed to evaluate how the micellar environment governs the interaction and conformational changes of Lo

* Corresponding author.
E-mail address: pietro@ffclrp.usp.br (P. Ciancaglini).

http://dx.doi.org/10.1016/j.jcis.2014.09.059
0021-9797/

and L_1 whereas molecular dynamics (MD) simulation allows for better describing the peptides location in the micelles.

2. Materials and methods

2.1. Material

All the solutions were prepared using Millipore Direct-Q ultra pure apyrogenic water. All reagents were of the highest commercially available purity grade; L-α-lysophosphatidylcholine (LPC), sodium dodecyl sulfate (SDS) and acrylamide were purchased from Sigma–Aldrich.

2.2. Peptide synthesis, cyclization and purification

Linear peptide L_1 (VWTVWGTIAG) was synthesized by Solid-Phase Peptide Synthesis procedure (SPPS) as previously described in Barbosa et al. [14]. After cleavage, Lo was obtained by L_1 cyclization. Peptides Lo and L_1 were purified by semi-preparative reversed phase HPLC C_{18} column and identified by electrospray mass spectrometry. All the details of the synthesis and purification processes are available in Barbosa et al. [14].

2.3. Circular dichroism (CD) spectroscopy

The CD spectra were recorded at 25 °C on a Jasco 810 spectropolarimeter. Lo or L_1, 100 μM, pH 7.0 were placed in a quartz cuvette with an optical path length of 0.1 cm and purged with nitrogen gas. Different concentrations of SDS (0–50 mM) or LPC (0–10 μM) were added to Lo or L_1, and each mixture was incubated for 30 min. The spectra were recorded from 250 to 190 nm, with 1 nm spectral bandwidth, scan speed of 100 nm min^{-1}, and 2 s time response, to minimize noise. The CD spectra correspond to the accumulation of ten runs after subtraction of the buffer spectrum.

2.4. Tryptophan fluorescence spectroscopy assays

Fluorescence was measured on a Spectronic SLM 8100 spectrofluorometer. Tryptophan groups were excited at 280 nm whereas the emission spectra were recorded from 300 to 500 nm, at 25 °C, pH 7.0 and quartz cells with optical path of 0.1 cm. The slit width at the excitation and the emission of the spectroflorimeter were 1 nm. The peptide emission spectra were subtracted from the peptide-free solution spectrum.

The fluorescence intensity and maximum wavelengths (λ_{max}) were obtained using an aqueous solution containing 10 μM of each peptide (Lo and L_1) in the absence and presence of different SDS concentrations (0–50 mM) and LPC (0–50 μM) varying a peptide/detergent mol ratio up to 2×10^{-4} and 2×10^{-1}, respectively.

Peptide interaction with micelles was also characterized by tryptophan fluorescence quenching by acrylamide, in the presence and absence of micelles, according to the Stern–Volmer equation:

$$Fo/F = 1 + K_{sv} \times [Q],$$

where Fo and F are the fluorescence intensities in the absence and presence of the quencher, respectively; $[Q]$ is the concentration of the quencher; and K_{sv} is the Stern–Volmer quenching constant. Fluorescence quenching measurements of tryptophan with the quencher were accomplished by adding aliquots (0.2 μL) of acrylamide stock solution (6 M) to a cuvette containing a fixed solution of peptide (10 μM) and another one with SDS and LPC solutions containing a peptide/detergent mol ratio of 2×10^{-3} and 5×10^{-3}, respectively.

2.5. Molecular dynamics simulation

The molecular dynamics (MD) studies were performed following the scheme represented in Fig. 1. To obtain the peptide–micelle complexes, the target systems were simulated by MD using coarse-grained (CG) representations of the molecules and the Martini force field [25,26]. Then, the atomistic structures of the peptide–micelle complexes were reconstructed from their corresponding CG representations using the algorithm developed by Rzepiela et al. [27]. Finally, the resulting systems were subjected to MD simulations with the GROMOS96 53a6 force field [28], for data analysis. All these simulations were carried out with the GROMACS 4.0.5 simulation package [29].

We conducted MD studies of linear and cyclic peptide with SDS and LPC micelles. For this purpose, CG systems containing the micelles in cubic boxes were prepared and equilibrated for 500 ns. A system was constructed with 60 SDS molecules, 60 Na^+ ions and 18,244 water molecules; another system was constructed with 100 LPC molecules and 24,740 water molecules. The force field parameters for the CG model of SDS were the same as those described by Jalili and Akhavan [30], while the parameters for LPC were derived from the DPPC force field [25]. Four other systems were then constructed from these systems, each containing a peptide, cyclic or linear, close to a micelle, SDS or LPC, and their water molecules and ions. Water molecules and ions superimposed with peptide atoms were removed, and the ions were added in new positions. For systems containing the linear peptide, one Na^+ and one Cl^- ion were inserted into electrostatically favorable positions, to neutralize the peptide charges. Simulations of these systems started with energy minimization using a steepest-descent algorithm, to eliminate bad contacts and undesirable forces. The MD simulations were carried out for 5 ns, with an integration time step of 10 fs; position restrictions were applied to the atomic coordinates of the peptides. Finally, all the restrictions were removed, and the simulations were carried out for 1 μs with time step of 30 fs, at 300 K. The parameters used in these simulations are the same described by Monticelli et al. [26] and are available at http://md.chem.rug.nl/marrink/coarsegrain.html.

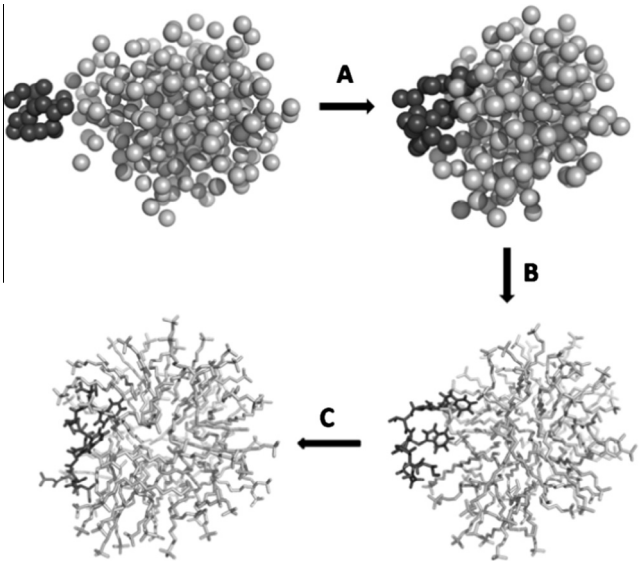

Fig. 1. Simulation scheme, considering the system containing the linear peptide with SDS micelle. The water molecules and ions have been removed for better visualization. (A) Formation of the peptide–micelle complex by CG simulation; (B) reconstruction of the atomic details of the peptide–micelle complex; (C) simulation of the complex with atomic details.

The atomistic structures of the peptide–micelle complexes, including a 0.5 nm layer of hydration water molecules and ions, were reversed from the final configurations obtained in the CG simulations. These systems were placed in the center of rhombic dodecahedron boxes and were completed with water molecules and ions. The bad contacts of these systems were eliminated by energy minimization using a steepest-descent algorithm. Next, simulations were conducted for 200 ps, with position restrictions for the peptide–micelle complexes. Simulations were then performed for 20 and 40 ns for the systems containing SDS and LPC micelles, respectively, with a time step of 2 fs. The force field parameters for SDS molecules were the same as those used in the work of Tummala and Striolo [31], and the parameters of the LPC molecules were derived from the DPPC molecule [32]. The SPC model [33] was used for the water molecules. The peptides and detergent covalent bonds were constrained by the LINCS algorithm [34], while the SETTLE algorithm [35] was used to keep rigid the SPC water molecules. The temperature of each system component was regulated separately by Berendsen's algorithm [36] using a correlation time of 0.1 ps. The pressure (1 bar) was controlled by pressure Berendsen's algorithm [36] (correlation time of 0.5 ps). A cutoff on the van der Waals was applied at 1.0 nm, and electrostatic interactions were evaluated by the particle mesh Ewald summation method [37]. The MD motion equations were integrated by the *leap-frog* algorithm [38].

3. Results and discussion

3.1. Fluorescence and CD results

The interaction of Lo and L_1 with micelles was first evaluated through changes occurring in the tryptophan (W) fluorescence emission in the presence of increasing SDS and LPC concentration below and above the critical micelle concentration, CMC [39–41]. Accordingly, the interaction between the peptides and SDS (Fig. 2A) promotes a blue-shift in the W maximum emission wavelength, λ_{max}, from aqueous solution (λ_{max} = 350 nm) to solution containing low amount of SDS (near CMC of 8 mmol/L [42]) amounting to 7 and 8 nm (Table 1) for Lo and L_1 peptides, respectively. Afterwards, the λ_{max} value remains constant at SDS concentrations higher than CMC. Of note, the fluorescence data refer to the emission of the two W residues present in the peptide structure (2nd and 5th residues). Therefore, the results give support to propose that the W residues of both peptides are surrounded by a more apolar environment in respect to water solution when in contact with the amphiphilic SDS molecule. This because a λ_{max} blue-shift is a fingerprint of changes from polar to apolar medium sensed by W residues [43–47]. In this way, a significant λ_{max} blue-shift indicates that the W residues, or at least one of them, must be buried in the hydrophobic core of the micelle. Of note, the W residues of the linear peptide seem to be slightly more inserted into the hydrophobic region of the SDS micelles than those of the cyclic form.

Furthermore, it is interesting to note that whereas in general an increase of the quantum yield is observed for such transitions, our results showed a decrease of it (data not shown) concomitantly with λ_{max} blue-shift. These data a decrease in the fluorescence intensity (data not shown) also took place, indicating conformational changes of the peptides [43,48] that came out in the presence of SDS micelle or also the interaction between the polar head of detergents and the W residues [46].

Referring to LPC-peptide interaction, λ_{max} underwent a blue shift of 5 and 2 nm, respectively, for Lo and L_1 peptides (Table 1) up to the addition of 5 μM LPC, with no alterations for higher LPC amount (Fig. 2B). Of note, the CMC value of LPC is around 7 μM [49]. Therefore, the λ_{max} blue shift indicated that the W residues of Labaditin experienced a lesser polar environment when the peptides interact with LPC micelles than with SDS micelles. The small λ_{max} blue shift observed when Labaditin is in contact with LPC points out that, probably, both forms of the peptide are not so embedded in the acyl-chain region of LPC micelles. The values obtained were quite low when compared with others peptides as Hylin-a1, for instance, that showed about 25 nm of shift

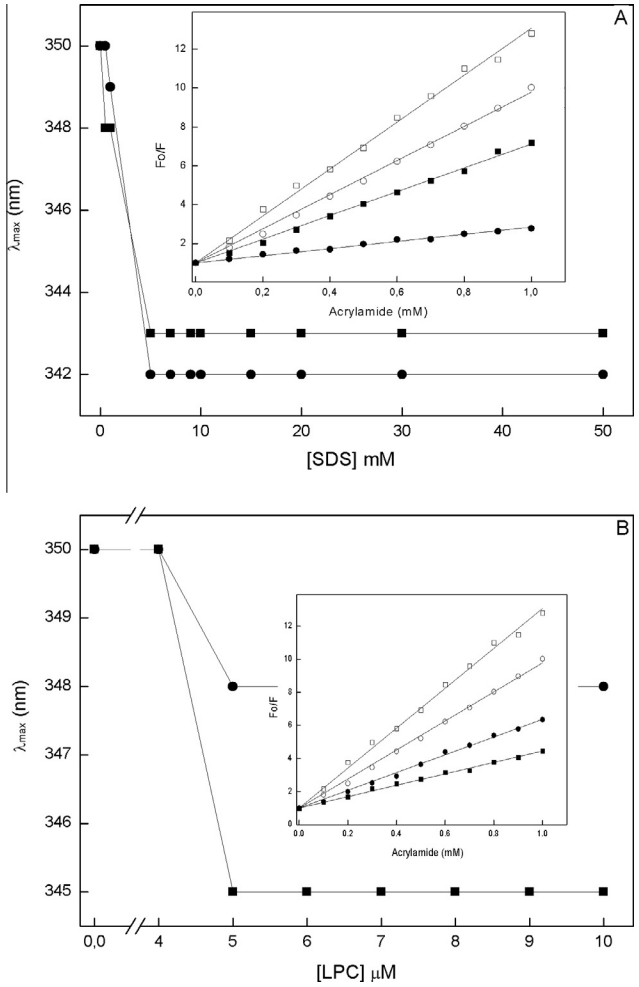

Fig. 2. Tryptophan λ_{max} emission from Lo (squares) and L_1 (circles) peptides (10 μM) in the presence of increasing SDS (A) and LPC (B) concentration (for details see Section 2). Inset: Fluorescence quenching (*Fo*/*F*) of the tryptophan residues present in Lo and L_1 in the absence (open symbols) and presence (full symbols) of amphiphile molecules, pH 7.0, by acrylamide quencher, according to Section 2.

Table 1
λ_{max} and K_{sv} values of Lo and L_1 in the absence (only water) and presence of SDS or LPC micelles. These parameters were obtained from Fig. 2. The experiments were conducted as described in Section 2.

Conditions	Parameter	Peptide	
		L_1	Lo
Water	λ_{max} (nm)	350	350
	K_{sv} (M^{-1})	8.8 ± 0.3	12.1 ± 0.6
SDS micelles	λ_{max} (nm)	342	343
	K_{sv} (M^{-1})	1.8 ± 0.1	6.1 ± 0.5
LPC micelles	λ_{max} (nm)	348	345
	K_{sv} (M^{-1})	5.4 ± 0.2	3.4 ± 0.1
DPPC liposomes[a]	λ_{max} (nm)	345	339
	K_{sv} (M^{-1})	4.8 ± 0.2	2.0 ± 0.1

[a] Data from Barbosa et al. [14].

[50–52]. Such finding suggests that the peptide must be located near the LPC micelle surface. This point will be better explored by MD later in the text.

Focusing on the acrylamide quenching results (insert in Fig. 2), the K_{sv} values (Table 1) revealed that the W residues of Lo (12.1 M^{-1}) are more exposed to the water than the W residues of L_1 (8.8 M^{-1}). The values of the extent of acrylamide quenching were much lower than Hylin-a1 or NATA in solution (almost 20 M^{-1}) that shown to be coiled in aqueous solution [53]. Addition of both SDS and LPC molecules decreased the K_{sv} values, revealing that the W residues of both Lo and L_1 became less accessed to the quencher. In the range of acrylamide used in this study, we obtained a linear fluorescence quenching dependence (inset in Fig. 2), indicating that both W residues, which are located in different positions of the peptide chain, are equally accessible to the quencher or only one W is most exposed to the surface and, hence, it must be quenched [39,45,46]. In a similar study performed with penetrating peptide from antennapedia, *a Drosophila*, the authors also examined the interaction of the peptide into membrane using quenching. The Stern–Volmer plots of the wild type peptide, which has two tryptophan residues, showed a linear slope too [45].

According to the K_{sv} data (Table 1), L_1 is more accessible to the acrylamide quencher when residing in the LPC micelle than in the SDS micellar aggregate [46]. Such observation reinforces the fact that the W residues of L_1 are experienced a more hydrophobic milieu in SDS micelle in respect to the LPC micelle as revealed by λ_{max} displacements. Further, Lo is less accessible to acrylamide in LPC micelles, although the corresponding λ_{max} blue-shift was on the same order as that found for SDS micelles (Table 1).

A comparison of the fluorescence results (Table 1) of both peptides on LPC micelles and DPPC large unilamellar vesicles previously reported [14] evidences that the Ws are lesser accessible to the acrylamide quencher and exposed to a lesser polar environment during interaction with DPPC vesicles than LPC micelles, albeit to a larger extent to Lo. Probably, such an effect may be attributed to differences in the phosphatidylcholine hydration shell which is higher in micelle environment, coupled to looser molecular packing.

With the aim of investigating the peptides conformational changes imparted by micelle interaction, far-UV CD spectroscopy was thereby employed. It is well known that the side chain of the amino acid W, indole group, displays four CD bands (La, Lb, Ba, and Bb). The La and Lb bands represent transitions to lower energies and appear in the region of 280 nm, so they are not visible in the Far-UV. The Ba and Bb bands correspond to higher-energy transitions. Depending on the conformation and location of the W residues, these bands can have either a positive or negative signal [54].

The CD spectrum of Lo in water, pH 7.0, had a negative band near 200 nm (Fig. 3A) which suggests an unordered peptide structure [14]. Addition of SDS caused changes in the CD spectrum of Lo (Fig. 3A), in a concentration-dependent manner, generating a band with maximum around 210 nm. Concerning to L_1, its spectrum in water at pH 7.0 displayed a minimum at approximately 198 nm and a maximum at ~224 nm, characteristic of a random coil structure [55]. This positive band is probably due to the proximity of both Trps giving rise to the interaction of their excited states [14,56,57]. The band in the 180–210 nm region represents a Ba transition, it is less intense than Bb, so it is not visible due to the strong band of L_1 in the same region (Fig. 3B). Addition of different concentrations of SDS changed the CD spectrum of L_1: a maximum at about 194 nm and a minimum at approximately 218 nm corresponding to β-sheet structure (Fig. 3B) took place. This alteration probably resulted from L_1-micelle interaction that separated the W residues, culminating in the loss of the band at 225 nm [56,58,59] due to the L_1 conformational change.

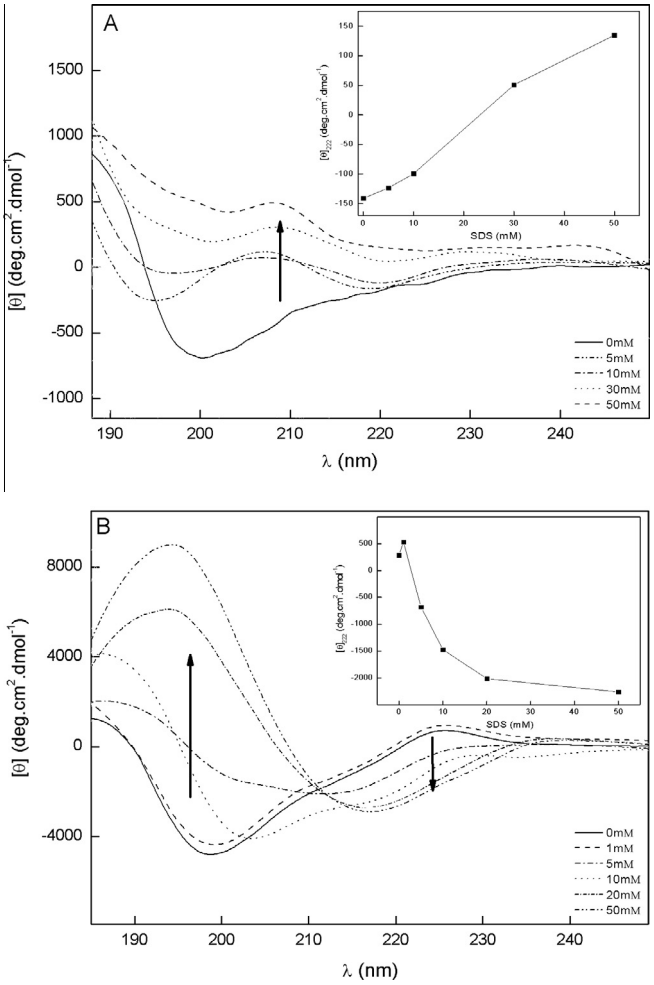

Fig. 3. Circular dichroism spectrum of Lo (A) and L_1 (B) at different SDS concentrations (from 0 to 50 mM), in aqueous medium, pH 7.0. The CD spectra were recorded as described in Section 2. Insets: relative change of CD signals at 222 nm as a function of the SDS concentration.

A similar study was done in the presence of LPC micelles (Fig. 4A). Structural changes of both peptides due to peptide-LPC interaction were observed. The CD spectrum of Lo in water, pH 7.0, displayed a negative band around 200 nm. Upon addition of LPC a positive band at 213 nm took place, in a concentration-dependent manner (Fig. 4B). The size and the cyclic structure of Lo confer a large conformational restriction, which promoted expressive modifications at low detergent concentrations near CMC. However, Lo still exhibited different CD spectra in SDS and LPC micelles (Figs. 3A and 4A), evidencing that it experienced different conformational changes in anionic and zwitterionic micelles.

In respect to L_1 in LPC micelles, pH 7.0, the band with maximum at ~224 nm disappeared (Fig. 4B), as observed for SDS (Fig. 3B). L_1 presented a negative band at 230 nm and a positive band at about 194 nm. It also showed a shoulder around 220 nm.

Note that the ellipticity at 222 nm (Inset of Figs. 3 and 4) as a function of concentration of detergent (interacting with both LPC and SDS micelle) results in a similar behavior, reducing and increasing the α-helix content for Lo and L_1, respectively. The highest change occurred in L_1 peptide, probably due to its linear structure.

These results demonstrated that different peptide structure conformations may occur for both peptides Lo and L_1 in the presence of LPC, evidencing that anionic and zwitterionic surfaces play

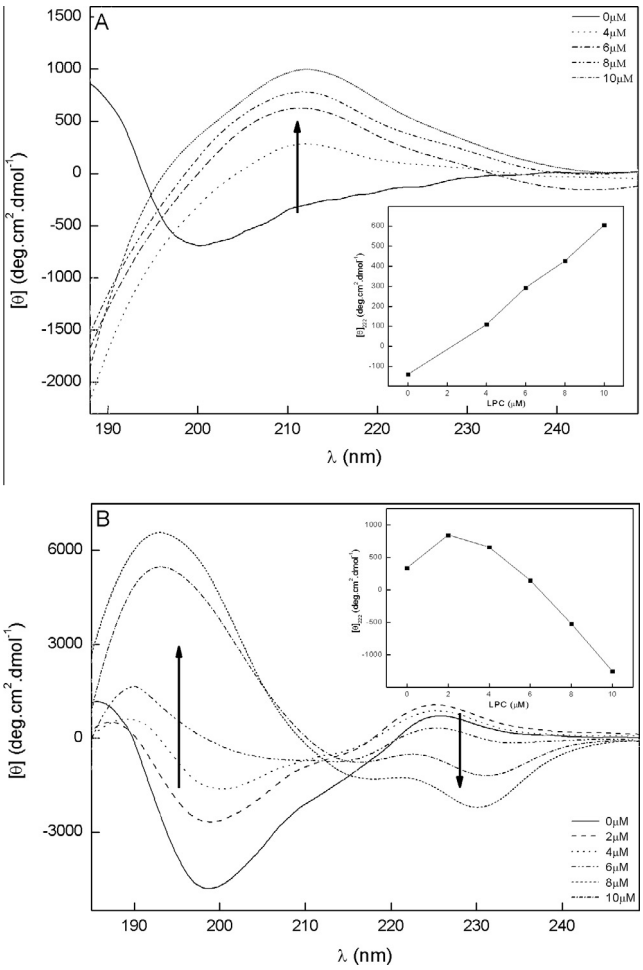

Fig. 4. Circular dichroism spectrum of Lo (A) and L_1 (B) at different concentrations of LPC (from 0 to 10 μM), in aqueous medium, pH 7.0. The CD spectra were recorded as described in Section 2. Insets: relative change of CD signals at 222 nm as a function of the LPC concentration.

an important role in the peptide/micelle interaction (hydrophobic and/or electrostatic forces), thus affecting the Labaditin conformation.

3.2. Study of Lo and L_1 interaction with micelles by MD simulations

The results of CG simulations demonstrated that Lo and L_1 peptides originally dispersed in water solution are driven to the micelle surroundings followed by their anchoring-insertion into the amphiphilic aggregate. By using force field with atomic details, both peptides also remained in the micelles (Fig. 5). In both SDS and LPC micelles L_1 peptide has a conformation that the tryptophan residues are almost facing each other, as suggested by CD (Fig. 3B). Differences will be detailed in the analysis of the trajectories performed during the simulations.

We calculated the C_α root-mean-square deviations for the C_α atoms of the peptides (RMSD) in relation to the initial structures obtained from the SDS simulations ($RMSD_{SDS}$) after back-mapping protocol. The behavior of $RMSD_{SDS}$ (Fig. 6A) showed that changes in the main chain occurred at the beginning of the simulations, indicating that the structures of the peptides Lo and L_1 obtained with the CG simulations were reorganized at atomic detail. Major changes in $RMSD_{SDS}$ did not take place thereafter, evidencing that the structures did not undergo major modifications during the SDS simulations.

We monitored the positions of the atoms of the peptides in the SDS micelles by calculating the radial distribution functions, $g_{SDS}(r)$, of all atoms from both Lo and L_1 peptides in respect to the micelle center of mass (CM) (Fig. 6B). The $g_{SDS}(r)$ of water molecules is also represented in Fig. 6B. Thus, one can note that water can penetrate until *circa* of 1.2 nm from the micelle CM, reminding that the SDS micelle core is around 1.6 nm with a polar head thickness of 0.5 nm [60]. The nonzero values of the $g_{SDS}(r)$ profiles of L_1 and Lo started from 0.25 and 0.80 nm, respectively, revealing that L_1 inserts part of its atoms deeper into the SDS micelle hydrophobic core than the cyclic peptide Lo.

The mean distances between the CM of each residue and the CM of the SDS micelles, d_{SDS} (Fig. 6C), evidenced that the N-terminal region of L_1 as well as all the residues to Ile8 are more inserted into

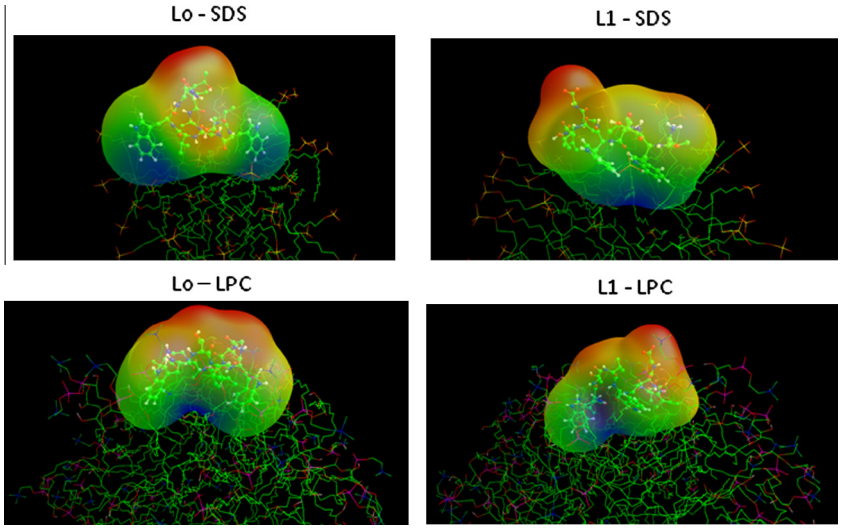

Fig. 5. Final configurations found for Lo and L_1 peptides interacting with micelles (SDS; top and LPC; bottom) by using force field with atomic details. The water molecules and ions have been removed for better visualization. SDS and LPC are represented in wireframe model. Peptides are represented in ball-stick model confined by polar surface area (PSA). In the PSA definition, apolar atoms are C and H bonded to C and polar atoms are O, S, N, P and H not bonded to C. Different colors on the surfaces are representing a polarity ruler: blue (more apolar), green (apolar), yellow (polar) and red (more polar). (For interpretation of the references to colour in this figure legend, the reader is referred to the web version of this article.)

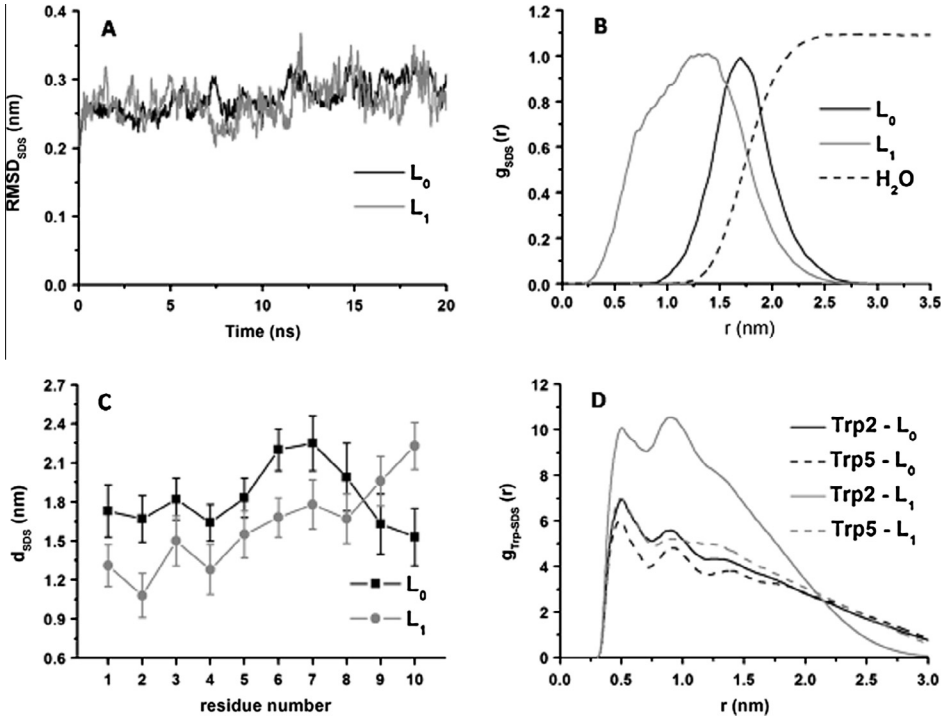

Fig. 6. (A) $RMSD_{SDS}$ of Lo and L_1 during the MD simulations showing the deviations of the structures in relation to the initial structure over time. (B) $g_{SDS}(r)$ of atoms of the peptides and water molecules to the CM of SDS micelles. The $g_{SDS}(r)$ of each peptide was normalized dividing the values by the maximum peak value. (C) Distance between the CM of the residues and the CM of the micelles. (D) Mean $g_{Trp\text{-}SDS}(r)$ between the C and N atoms of W side chains and the carbon atoms of the SDS tails. The data contained in A, B, and C were calculated from 10 to 20 ns.

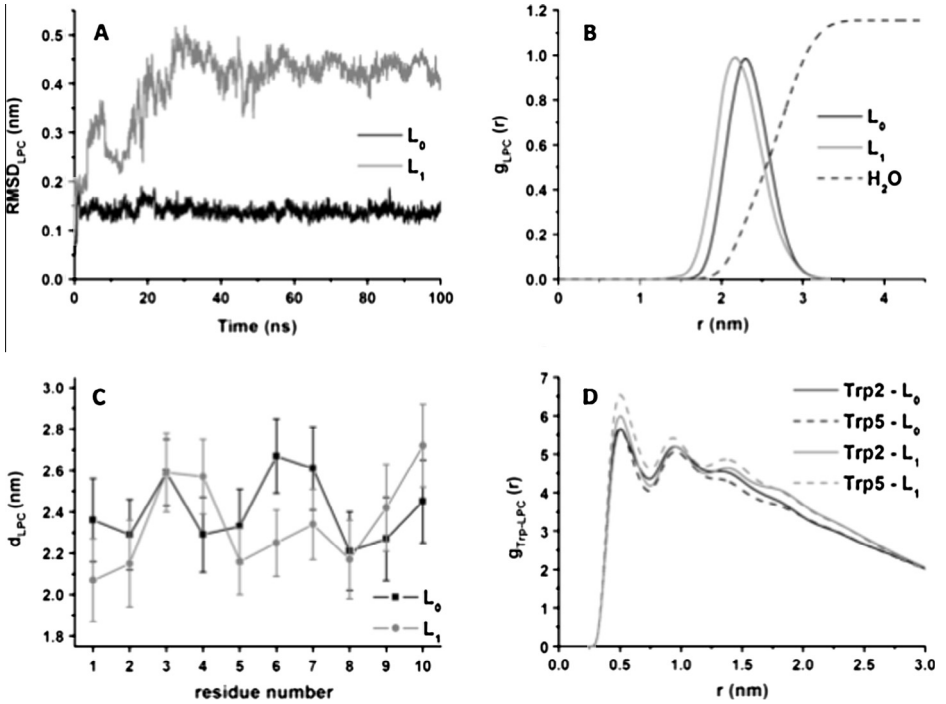

Fig. 7. (A) $RMSD_{LPC}$ of Lo and L_1 during the MD simulations showing the deviations of the structures in relation to the initial structure over time. (B) $g_{LPC}(r)$ of atoms of the peptides and water molecules to the CM of LPC micelles. The $g_{LPC}(r)$ of each peptide was normalized dividing the values by the maximum peak value. (C) Distance between the CM of the residues and the CM of the micelles. (D) Mean $g_{Trp\text{-}LPC}(r)$ between the C and N atoms of W side chains and the carbon atoms of the LPC tails. The data contained in A, B, and C were calculated from 50 to 100 ns.

the hydrophobic core of the micelle than those of Lo. The deepest inserted residue is W2, suggesting that this amino acid residue drives insertion of the N-terminal region of L_1 into the SDS micelles. Such a result explains the fluorescence data: the fluorescence and quenching experiments suggest that L_1 is more buried into the SDS micelles than Lo (Fig. 2A and Table 1). The simulation data also revealed that the W5 residues of both Lo and L_1 are located in similar environmental of the micelle; therefore, the

differences observed in the fluorescence spectra are due to the deeper insertion of W2 of the linear peptide into micelle.

To emphasize that the W2 residue of L_1 interacts indeed with the hydrophobic core of the micelle, we calculated the mean radial distribution function $g_{Trp\text{-}SDS}(r)$ from the pairs formed between the C or N atoms of the W residues side chain and the carbon atoms of the hydrophobic chains of the SDS molecules. The results are shown in Fig. 6D. The well-defined first peak of $g_{Trp\text{-}SDS}(r)$ of the W2 residue from the L_1 peptide at 0.48 nm indicated that the W side chain is surrounded by Carbon atoms of the hydrophobic core. Therefore, the W2 residue of L_1 is indeed located into the hydrophobic region of the SDS micelle. Noteworthy, regardless where the L_1 and Lo reside in the micelle, Labaditin undergoes conformational changes driven by its interaction in the micelle-like aggregates as clearly observed by CD experiments (Fig. 4).

Concerning LPC micelles, the $RMSD_{LPC}$ values (Fig. 7A) indicated that the Lo main chain had a quite small variation with time: the alterations were around 0.15 nm during the simulation. Major modifications occurred in the main chain of L_1 during the simulation – values up to 0.48 nm were obtained at 30 ns; a convergence behavior was reached only at 50 ns. Hence, the use of a force field with all atomic details led to an unequal structure of the linear peptide in the LPC micelle when compared to the CG simulation. Fig. 7B shows the radial distribution function $g_{LPC}(r)$ between peptides and water in relation to the CM of the LPC micelle. As seen in the same figure, $g(r)$, the water can penetrate until *circa* of 1.6 nm from the micelle CM, L_1 and Lo for 1.4 nm and 1.5 nm, respectively, are mainly located close to the apolar/polar interface, i.e., to the zwitterionic polar head [61]. The d_{LPC} results (Fig. 7C) evidenced that the major differences in the peptides location occurred for the regions containing the 1st and 2nd residues and the 5th to 7th residues, which include W residues, thus justifying the small λ_{max} blue-shifts detected from the fluorescence emission experiments (Fig. 2B and Table 1).

To observe the differences between the behavior of the W residues of L_1 and Lo, we now calculated their interaction with LPC micelles. The aromatic side chain of the W residues of L_1 exhibited slightly more intense peaks for the $g_{Trp\text{-}LPC}(r)$ profiles between the side chain C and N atoms and the carbon atoms of the LPC hydrophobic tails (Fig. 7D). The peaks appeared at 0.48 nm, as observed in the SDS results, indicating that there are contacts with the tail carbon atoms, although to a lesser extent than in the case of SDS (Fig. 6D). This happens because the W residues are not deeply inserted into the hydrophobic core of the LPC micelle as it was demonstrated for SDS micelles.

4. Conclusion

Combined results from experimental fluorescence and CD data as well as MD simulations provided information on micelle–peptide interaction. Both Lo and L_1 peptides undergo conformational changes from aqueous to micelle (SDS and LPC) environment. Lo presents unordered structure whereas L_1 changes its conformation from random coil to β-structure in the presence of micelles. The linear peptide inserts deeper in the hydrophobic region into SDS micelles than does the cyclic one. Comparing the interaction of both peptides with LPC micelles and DPPC vesicles, we observed that Lo and L_1 are located preferentially at the micelle–water interface in the former case and are more inserted in the hydrophobic region in the latter case. Probably, changes in the lipid hydration layer due to differences in membrane curvature and the delicate balance between hydrophobic and hydrophilic components must play the key role in determining the peptide insertion in the PC-model membrane. Interestingly, in the presence of negatively charged membranes, the linear peptide prefers to reside deeper in the hydrophobic core in contrast to its location nearest to zwitterionic interfaces.

Acknowledgments

We are grateful to Conselho Nacional de Desenvolvimento Científico e Tecnológico (CNPq), FAPESP, rede CYTED and Coordenação de Aperfeiçoamento de Nível Superior – Project NanoBiotec (CAPES) for financial support. We thank Cynthia Maria de Campos Prado Manso and Priscila Cerviglieri for linguistic advice. PC, EMC, RI, and RGS are CNPq researchers, and SCB received a PhD fellowship from CAPES.

References

[1] Y.U. Kwon, T. Kodadek, Chem. Biol. 14 (2007) 671.
[2] Q. Xiao, D. Pei, J. Med. Chem. 50 (2007) 3132.
[3] G.A. Grant (Ed.), Synthetic Peptides: A Users's Guide, Oxford University Press, Inc., New York, 2002.
[4] Z. Qian, T. Liu, Y.Y. Liu, R. Briesewitz, A.M. Barrios, S.M. Jhiang, D. Pei, ACS Chem. Biol. 8 (2013) 423.
[5] T. Rezai, J.E. Bock, M.V. Zhou, C. Kalyanaraman, R.S. Lokey, M.P. Jacobson, J. Am. Chem. Soc. 128 (2006) 14073.
[6] T. Rezai, B. Yu, G.L. Millhauser, M.P. Jacobson, R.S. Lokey, J. Am. Chem. Soc. 128 (2006) 2510.
[7] A.T. Bockus, C.M. McEwen, R.S. Lokey, Curr. Top. Med. Chem. 13 (2013) 821.
[8] N.H. Tan, J. Zhou, Chem. Rev. 106 (2006) 840.
[9] X.P. Zhang, M.L. Zhang, X.H. Su, C.H. Huo, Y.C. Gu, Q.W. Shi, Chem. Biodivers. 6 (2009) 2166.
[10] D.G. Picchi, W.F. Altei, M.S. Saito, V.S. Bolzani, E.M. Cilli, Quim. Nova 32 (2009) 1262.
[11] C. Auvin, C. Baraguey, A. Blond, F. Lezenven, J.L. Pousset, B. Bodo, Tetrahedron Lett. 38 (1997) 2845.
[12] C.J. Barber, P.T. Pujara, D.W. Reed, S. Chiwocha, H. Zhang, P.S. Covello, J. Biol. Chem. 288 (2013) 12500.
[13] P.G. Arnison, M.J. Bibb, G. Bierbaum, A.A. Bowers, T.S. Bugni, G. Bulaj, J.A. Camarero, D.J. Campopiano, G.L. Challis, J. Clardy, P.D. Cotter, D.J. Craik, M. Dawson, E. Dittmann, S. Donadio, P.C. Dorrestein, K.D. Entian, M.A. Fischbach, J.S. Garavelli, U. Goransson, C.W. Gruber, D.H. Haft, T.K. Hemscheidt, C. Hertweck, C. Hill, A.R. Horswill, M. Jaspars, W.L. Kelly, J.P. Klinman, O.P. Kuipers, A.J. Link, W. Liu, M.A. Marahiel, D.A. Mitchell, G.N. Moll, B.S. Moore, R. Muller, S.K. Nair, I.F. Nes, G.E. Norris, B.M. Olivera, H. Onaka, M.L. Patchett, J. Piel, M.J. Reaney, S. Rebuffat, R.P. Ross, H.G. Sahl, E.W. Schmidt, M.E. Selsted, K. Severinov, B. Shen, K. Sivonen, L. Smith, T. Stein, R.D. Sussmuth, J.R. Tagg, G.L. Tang, A.W. Truman, J.C. Vederas, C.T. Walsh, J.D. Walton, S.C. Wenzel, J.M. Willey, W.A. van der Donk, Nat. Prod. Rep. 30 (2013) 108.
[14] S.C. Barbosa, E.M. Cilli, L.G. Dias, R.G. Stabeli, P. Ciancaglini, Amino Acids 40 (2011) 135.
[15] S. Kosasi, W.G. Vandersluis, R. Boelens, L. Thart, R.P.L. Labadie, FEBS Lett. 256 (1989) 91.
[16] C.W. Sabandar, N. Ahmat, F.M. Jaafar, I. Sahidin, Phytochemistry 85 (2013) 7.
[17] R.P. Labadie, S.M. Colegate, R.J. Molyneux (Eds.), Bioactive Natural Products, CRC Press, Boca Raton, Ann Arbor, London, Tokyo, 1993.
[18] L.M. Gierasch, J.E. Lacy, K.F. Thompson, A.L. Rockwell, P.I. Watnick, Biophys. J. 37 (1982) 275.
[19] I.L. Bermejo, C. Arnulphi, A. Ibanez de Opakua, M. Alonso-Marino, F.M. Goni, A.R. Viguera, Biophys. J. 105 (2013) 1432.
[20] E.S. Rowe, F. Zhang, T.W. Leung, J.S. Parr, P.T. Guy, Biochemistry 37 (1998) 2430.
[21] T. Imamura, K. Konishi, J. Pept. Sci. 12 (2006) 403.
[22] H. Sun, D.V. Greathouse, O.S. Andersen, R.E. Koeppe 2nd, J. Biol. Chem. 283 (2008) 22233.
[23] A.A. Gorfe, R. Baron, J.A. McCammon, Biophys. J. 95 (2008) 3269.
[24] G. Bach, L. Perrin-Cocon, E. Gerossier, A. Guironnet-Paquet, V. Lotteau, G. Inchauspe, A. Fournillier, Clin. Vaccine Immunol. 17 (2010) 429.
[25] S.J. Marrink, H.J. Risselada, S. Yefimov, D.P. Tieleman, A.H. de Vries, J. Phys. Chem. B 111 (2007) 7812.
[26] L. Monticelli, S.K. Kandasamy, X. Periole, R.G. Larson, D.P. Tieleman, S.J. Marrink, J. Chem. Theory Comput. 4 (2008) 819.
[27] A.J. Rzepiela, L.V. Schäfer, N. Goga, H.J. Risselada, A.H. De Vries, S.J. Marrink, J. Comput. Chem. 31 (2010) 1333.
[28] C. Oostenbrink, A. Villa, A.E. Mark, W.F. van Gunsteren, J. Comput. Chem. 25 (2004) 1656.
[29] B. Hess, C. Kutzner, D. Van der Spoel, E. Lindahl, J. Chem. Theory Comput. 4 (2008) 435.
[30] S. Jalili, M. Akhavan, Biophys. Chem. 153 (2011) 179.
[31] N.R. Tummala, A. Striolo, J. Phys. Chem. B 112 (2008) 1987.
[32] A. Kukol, J. Chem. Theory Comput. 5 (2009) 615.
[33] H.J.C. Berendsen, J.R. Grigera, T.P. Straatsma, J. Phys. Chem. 91 (1987) 6269.
[34] B. Hess, H. Bekker, H.J.C. Berendsen, J.G.E.M. Fraajie, J. Comput. Chem. 18 (1997) 1463.

[35] S. Miyamoto, P.A. Kollman, J. Comput. Chem. 13 (1992) 952.
[36] H.J.C. Berendsen, J.P.M. Postma, A. DiNola, J.R. Haak, J. Chem. Phys. 81 (1984) 3684.
[37] T. Darden, D. York, L. Pedersen, J. Chem. Phys. 98 (1993) 10089.
[38] R.W. Hockney, S.P. Goel, J. Eastwood, J. Comput. Phys. 14 (1974) 148.
[39] M.R. Eftink, C.A. Ghiron, Biochemistry 15 (1976) 672.
[40] R. Gopal, J.H. Lee, Y.G. Kim, M.S. Kim, C.H. Seo, Y. Park, Mar. Drugs 11 (2013) 1836.
[41] C. Zhang, C. Gao, J. Mu, Z. Qiu, L. Li, Biomed. Res. Int. 2013 (2013) 349542.
[42] H. Xu, P.X. Li, K. Ma, R.K. Thomas, J. Penfold, J.R. Lu, Langmuir: ACS J. Surf. Colloid 29 (2013) 9335.
[43] Y. Chen, M.D. Barkley, Biochemistry 37 (1998) 9976.
[44] R. Gopal, J.K. Lee, J.H. Lee, Y.G. Kim, G.C. Oh, C.H. Seo, Y. Park, Int. J. Mol. Sci. 14 (2013) 2190.
[45] B. Christiaens, S. Symoens, S. Verheyden, Y. Engelborghs, A. Joliot, A. Prochiantz, J. Vandekerckhove, M. Rosseneu, B. Vanloo, S. Vanderheyden, Eur. J. Biochem. 269 (2002) 2918.
[46] J.R. Lakowicz, Principles of Fluorescence Spectroscopy, third ed. Springer, New York, 2006, p. 395.
[47] O. Azimi, Z. Emami, H. Salari, J. Chamani, Molecules 16 (2011) 9792.
[48] S. Jana, T.K. Chaudhuri, J.K. Deb, Biochem. Biokhim. 71 (2006) 1230.
[49] R.E. Stafford, T. Fanni, E.A. Dennis, Biochemistry 28 (1989) 5113.
[50] E. Crusca, A.A. Rezende, R. Marchetto, M.J. Mendes-Giannini, W. Fontes, M.S. Castro, E.M. Cilli, Biopolymers 96 (2011) 41.
[51] R.F. Vieira, F. Casallanovo, N. Marín, A.C. Paiva, S. Schreier, C.R. Nakaie, Biopolymers 92 (2009) 525.
[52] T.A. Pertinhez, C.R. Nakaie, A.C. Paiva, S. Schreier, Biopolymers 42 (1997) 821.
[53] I.F. Pazos, D. Martinez, M. Tejuca, A. Valle, A. del Pozo, C. Alvarez, M.E. Lanio, E.A. Lissi, Toxicon 42 (2003) 571.
[54] I.B. Grishina, R.W. Woody, Faraday Discuss. (1994) 245.
[55] A.S. Ladokhin, S. Jayasinghe, S.H. White, Anal. Biochem. 285 (2000) 235.
[56] R.W. Woody, Theory of Circular Dichroism of Protein, Plenum Press, New York, 1996.
[57] J.J. Yang, M. Pikeathly, S.E. Radford, Biochemistry 33 (1994) 7345.
[58] M.L. Sforça, A. Machado, R.C. Figueredo, S. Oyama, F.D. Silva, A. Miranda, S. Daffre, M.T. Miranda, A. Spisni, T.A. Pertinhez, Biochemistry 44 (2005) 6440.
[59] D. Andersson, U. Carlsson, P. Freskgard, Eur. J. Biochem. 268 (2001) 1118.
[60] R. Itri, L.Q. Amaral, Phys. Rev. E 47 (1993) 2551.
[61] L.R. Barbosa, W. Caetano, R. Itri, P. Homem-de-Mello, P.S. Santiago, M. Tabak, J. Phys. Chem. B 110 (2006) 13086.